

Published: December 31, 2023

Citation: Marneffe A, Van Simaey G, et al., 2023. In vivo non-invasive skin imaging of cutaneous involvement in systemic sclerosis, Medical Research Archives, [online] 11(12).

<https://doi.org/10.18103/mra.v11i12.4440>

Copyright: © 2023 European Society of Medicine. This is an open-access article distributed under the terms of the Creative Commons Attribution License, which permits unrestricted use, distribution, and reproduction in any medium, provided the original author and source are credited.

DOI

<https://doi.org/10.18103/mra.v11i12.4440>

ISSN: 2375-1924

RESEARCH ARTICLE

In vivo non-invasive skin imaging of cutaneous involvement in systemic sclerosis

Marneffe Alice¹, M.D; Van Simaey Gaetan², PhD; Vanholsbeeck Frédérique³, PhD; Sarrand Julie⁴, M.D; Woods Daniel¹, PhD; #Del Marmol Véronique¹, M.D, PhD; #Soyfoo Muhammad⁴, M.D, PhD

¹ Department of Dermatology, Hôpital Erasme, Université libre de Bruxelles, Belgium

² Department of Nuclear imaging, Hôpital Erasme, Université libre de Bruxelles, Belgium

³ Department of Physics, University of Auckland, New Zealand, The Dodd Walls Centre for photonics and quantum technologies, New Zealand

⁴ Department of Rheumatology, Hôpital Erasme, Université libre de Bruxelles, Belgium

contributed equally to the article

***Corresponding author:** M.S Soyfoo, M.D, Ph.D

Professor of Rheumatology, ULB

Head of Department Rheumatology, Hôpital Erasme

Email : msoyfoo@ulb.ac.be

Note: Dr del Marmol and Dr Soyfoo contributed equally to this paper

ABSTRACT

Objectives: To evaluate the diagnostic and prognostic value of quantitative biomarkers derived from optical coherence tomography measurements for the management of patients with systemic sclerosis and to compare their clinical utility with the modified Rodnan skin score (mRSS).

Methods: Thirty-seven patients and 38 healthy volunteers were selected. The mRSS was performed in both groups over 17 anatomical sites and optical coherence tomography images were obtained over 7 of the 17 anatomical sites using 2 commercially available systems. For all sites, both types of images were processed to quantify the optical absorption, area and thickness of the different layers of the skin.

Results: For both systems, the 3 most extreme results and usually more affected locations provided statistically relevant data. For one system, the dermal-epidermal junction area, i.e. the integral sum of the optical density, led to significant difference between both groups. For the other system, the junction slope, i.e. the optical density gradient, demonstrated an excellent accuracy in scleroderma diagnosis when mRSS was high in the most relevant lesions, and superior sensitivity and specificity when mRSS was low.

Conclusions: This study shows promising results for optical coherence tomography to provide an objective non-invasive examination tool for early diagnosis of systemic sclerosis.

Keywords: systemic sclerosis, skin, imaging, optical coherence tomography

Introduction

Systemic sclerosis (SSc) is a rare and heterogeneous autoimmune connective tissue disease characterized by fibroproliferative vasculopathy, inflammation and aberrant fibrosis of the skin and internal organs, ensuing progressive impairment and failure of the affected organs¹⁻³. SSc is classically divided in two distinct subsets based on the pattern of skin involvement^{1,4}. Limited cutaneous SSc (lcSSc) is usually delineated by limited skin fibrosis and vascular manifestations whereas diffuse cutaneous SSc (dcSSc) is dominated by a rapidly progressive and widespread fibrosis of the skin and internal organs, often associated with a disastrous prognosis despite the considerable progress made in the management of patients and the understanding of the underlying pathophysiology^{5,6}. Even though progressive skin thickening is a dominant feature of the disease, internal organs fibrosis mainly affects the clinical outcome and prognosis^{7,8}. The severity of skin fibrosis and its progression rate are assessed by the modified Rodnan skin score (mRSS), a semi-quantitative evaluation of skin stiffness at seventeen body sites⁹. mRSS is a tool of pivotal importance in the management of the disease as it's considered as a surrogate marker of disease severity (i.e. systemic organ involvement) and mortality¹⁰⁻¹³. Despite being currently considered as the gold standard for assessing SSc patients, mRSS has several limitations due to operator skills and interpretations^{14,15}. Skin biopsy has not been validated for the diagnosis of SSc due to delayed healing and scarring in SSc patients^{6,16}.

Due to the lack of validated and objective skin assessment tools in SSc, several non-invasive diagnostic modalities such as dermoscopy¹⁷, durometry^{18,19} and high frequency ultrasonography (HFUS)^{20,21} have emerged over the last years as alternative diagnosis and management tools. These techniques allow the non-invasive visualization of the morphological changes of the skin that are not visible to the naked eye, both in real-time and over-time, and has been advocated as promising tools in evaluating skin involvement in SSc²²⁻²⁴.

In recent years, optical coherence tomography (OCT) has been introduced. OCT is a real time non-invasive imaging technique allowing imaging of three-dimensional volume of tissue and producing high resolution and contrasts images of superficial layers of the skin²⁵. It is currently used in ophthalmology for the diagnosis of retinal diseases²⁶ as well as in cardiology²⁷ and dermatology²⁸. By generating cross-sectional images of tissue, OCT enables visualization of altered skin architecture present in superficial skin lesions²⁸. Promising results have been demonstrated

mainly for non-melanoma skin cancers²⁹. Several systems have been commercialized over the last decade with different resolutions, penetration depth and, therefore, clinical applicability^{30,31}. A first study assessed the ability of OCT to detect and quantify skin fibrosis in SSc. OCT imaging correlated with histological skin changes. Moreover, a high mRSS was associated with a progressive loss of visualization of the dermal-epidermal junction and a decrease of the optical density in the papillary dermis. The intra-observer and inter-observer reliability was high, but the sample included only a small number of patients with similar degrees of fibrosis³²⁻³⁴.

The aim of this study is to evaluate the use of OCT for the diagnosis and therapeutic monitoring in SSc using two commercially available OCT systems optical coherence tomography.

Methods

PATIENTS

Forty-two SSc patients followed in Erasmus Hospital were enrolled in the study. Thirty-eight of them fulfilled the American College of Rheumatology/European League Against Rheumatism (ACR/EULAR) classification criteria for SSc and were included in the study. Thirty-eight healthy volunteers were recruited from the staff. Clinical and demographic data were gathered. mRSS evaluation was performed by a fully trained rheumatologist and was executed independently of the OCT evaluation. The study was approved by the local ethics committee of Erasmus Hospital. All patients and controls signed a written informed consent to participate in the study.

IMAGING

OCT scans was performed in all patients and healthy volunteers at 7 of the 17 anatomical sites used for the mRSS, namely first phalanx, second phalanx, dorsal aspect of the hand, posterior aspect of the forearm, posterior aspect of the arm, neckline and face, all calculated on the left side. The OCT scans were performed using the "Vivosight®" multi-beam OCT probe (Michelson Diagnostics) and the "Skintell®" high-definition (HD)-OCT probe (Agfa Healthcare Mortsels, Belgium and München, Germany). Those two OCT scans were used because of the complementary information they provide. Vivosight® enables vertically oriented imaging of the skin from the surface up to 2 mm, reaching higher penetration depth than the Skintell®, but is characterized by a lower lateral resolution (7,5 µm) (figure 1A). Skintell® is characterized by a higher resolution of 6 µm sufficient to provide cellular visualization, enables real-time and dynamic three-dimensional imaging of the skin from the surface up

to 570 μ m (papillary dermis) (figure 1B). Acquisition procedures are described in detail elsewhere^{32,35}.

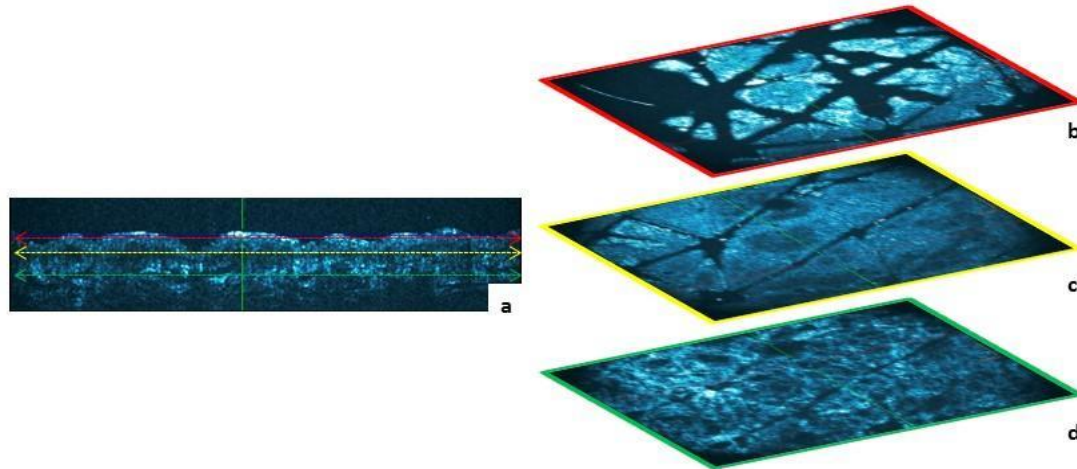


Figure 1A. HD-OCT enables 3-D imaging of the skin providing both (a) cross sectional images and en face images through (b) the stratum corneum, (c) the epidermis, (d) to the reticular dermis.
Abbreviations: HD-OCT: high-definition optical coherence tomography

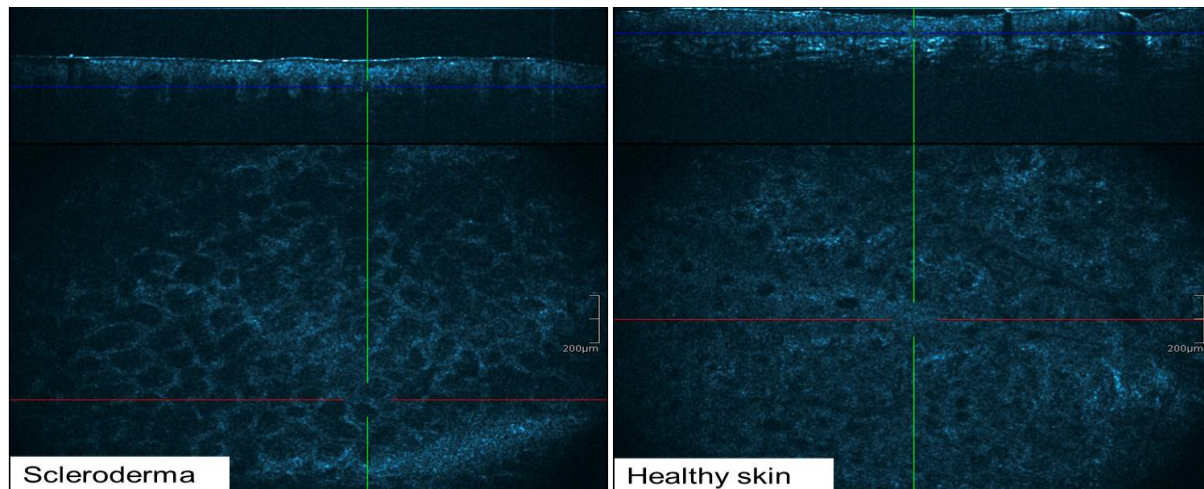


Figure 1B. Comparison of cutaneous involvement in systemic sclerosis and normal skin imaged with HD-OCT
Abbreviations: HD-OCT: high-definition optical coherence tomography

IMAGE PROCESSING

Multi-Beam OCT: Vivosight®

The A-scans i.e. the OCT signal plotted at each lateral position against depth-in-tissue, were averaged over the entire volume using the same custom processing written in Matlab (2012a, The MathWorks, Natick, MA, USA) previously reported elsewhere³². The image processing is going through these successive steps: (1) the skin surface is detected and is set at the same level (i.e. corrected depth) in the whole image volume so as to correct for natural or patient-related variations; (2) the optical density (OD) through the skin depth is normalized relative to the OD at the skin surface; (3) the data at each corrected depth beneath the skin surface are averaged. Apart from the air-skin interface, where the difference in refractive index causes an intensity peak, the obtained mean A-scan

exhibits a monotonic decay of the signal, with the noticeable exception of the papillary dermis (PD) that appears hyper-reflective, in contrast to the hypo-reflective dermal-epidermal junction (DEJ), which produces a valley. The distance between the skin surface and the DEJ corresponds to the epidermis thickness (ET), while a bulge in the OCT signal beyond the epidermis characterizes the transition from the epidermis to the PD. The processing automatically extracts these A-scan features by performing the following measurements: (1) the junction thickness (JT), corresponding to the distance between the DEJ and the skin depth at which the same OD as the one observed at the DEJ is found in the PD; (2) the junction OD (JOD), corresponding to the difference in OD between PD peak and DEJ valley; (3) the junction area (JA), corresponding to the integral sum

of the OD in the whole “bulge” thickness; (4) the junction slope (JS), defined as the maximum OD gradient found after the DEJ, limited to the first 400 μm of tissue.

High-definition OCT: Skintell®

The quantification of the volumetric images was performed with a custom-made interface written in LabView® (Labview2011; National Instruments,

Austin, TX, USA. An average intensity profile is calculated over a skin area of 150 μm by 150 μm (50 by 50 pixels) selected using the images at 30 μm depth above and below the plane with the highest backscattering intensity, in the papillary and reticular dermis respectively (figure 2). The volume was chosen to include regular and homogeneous structures.

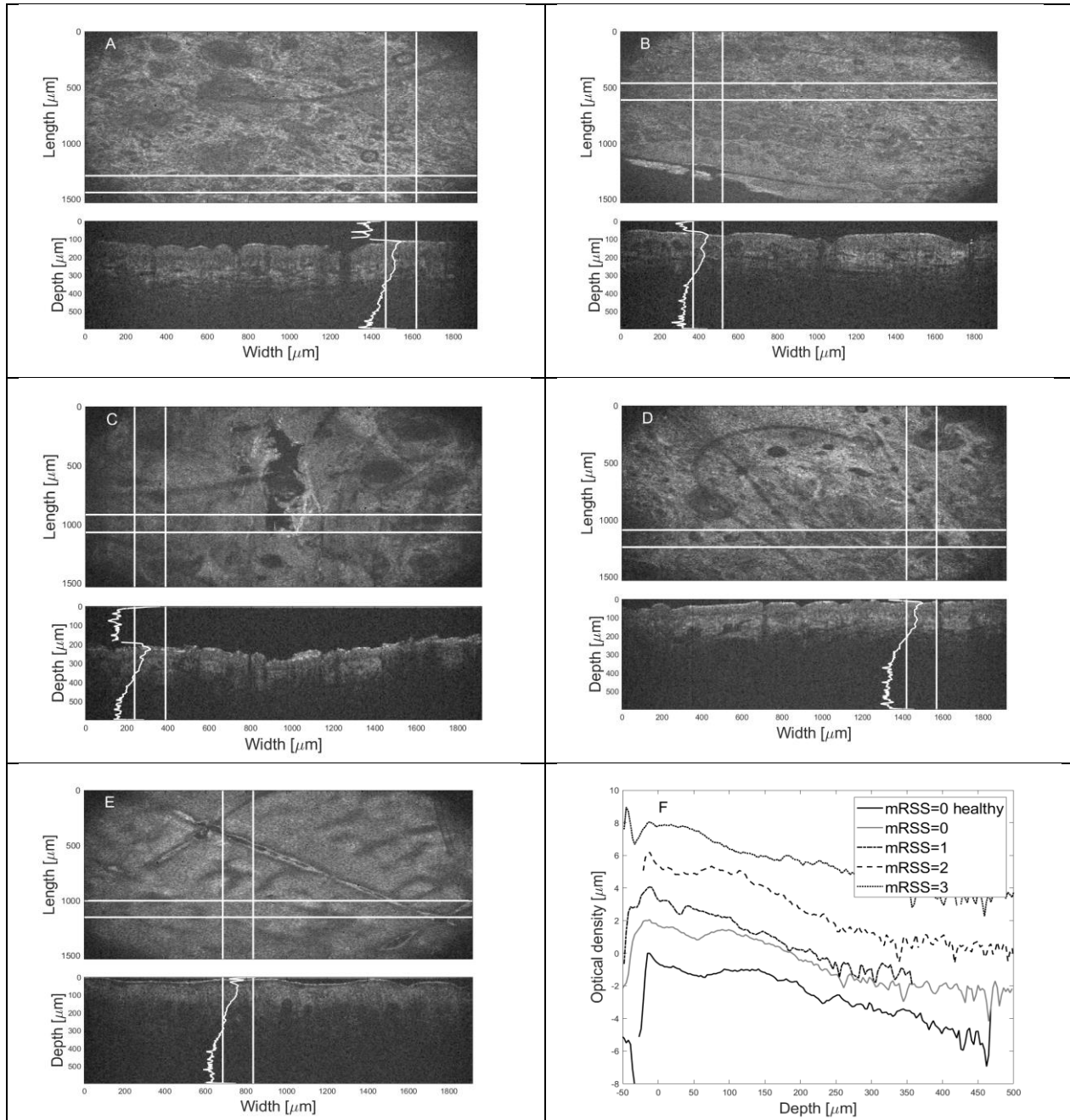


Figure 2. Example of image processing with the Skintell data set for location 2 for (A) a healthy volunteer (mRSS=0) and for SSc patients displaying a Rodnan score of (b) mRSS=0, (C) mRSS=1, (d) mRSS=2 and (e) mRSS=3. Insert F shows all the depth profiles displaced vertically for the sake of clarity of display.

Abbreviations: mRSS: modified Rodnan skin score

Three out of the four parameters studied with the Vivosight® OCT, namely, JT, JOD and JS, were

obtained by manual location and measurement of the relevant features in the average A-scan profiles

from the Skintell® data. Additional parameters were investigated with the Skintell®, i.e., the epidermis-dermis distance, epidermis and PD attenuation (both absolute and normalized to the maximum in profile), and PD-to-epidermis attenuation ratio.

STATISTICAL ANALYSIS

Statistical analyses were performed using GraphPad Prism 7.0b (GraphPad Software, La Jolla, CA, USA). The correlations of each of the four quantitative parameters derived from both Vivosight and Skintell with mRSS were performed using nonparametric Spearman's correlations (Rodnan index is neither continuous nor normally distributed) and their significance was assessed by means of the associated two-tailed P value. The patient and control groups were compared location per location using unpaired two-tailed parametric t tests. As we compared different quantitative parameters for different locations, multiple parametric comparisons were performed without assuming a consistent standard deviation (SD), but P-values were corrected for multiple comparisons with the Holm-Šídák method. The statistical significance level was set to 0.05 throughout the analyses. Receiver Operator Characteristic (ROC) curves were derived for every statistically significant parameter with both OCT systems in each of the 7 investigated lesions. Area under the

curve (AUC) and its corresponding P-value were estimated, as well as the cutoff value and associated sensitivity and specificity provided AUC was higher than 0.75. ROC curves were similarly obtained for mRSS to compare its classification performance with the quantitative OCT parameter. Beside these correlations, t tests and ROC curves applied for all patients, additional correlations, multiple t tests and ROC curves were performed and computed with the sole patients with mRSS equal to 0 for the few quantitative parameters that proved to be statistically relevant with the previous tests, so as to assess the clinical utility of the elicited OCT-derived parameters against the mRSS.

Results

PATIENTS AND CONTROLS

A total of thirty-eight patients were included in the study and fulfilled the American College of Rheumatology/European League Against Rheumatism (ACR/EULAR) classification criteria for SSc³⁶. Among them, 28 patients had a limited SSc and 10 had a diffuse SSc according to LeRoy and Medsger³⁷. Thirty-eight healthy volunteers who matched for age and phototype, without dermatologic disease, were recruited as controls. The epidemiological and clinical data are summarized in Table 1. We obtained 532 volumes with each imaging technique.

Table 1. Demographic, clinical, laboratory data of 38 SSc patients and 38 healthy controls.

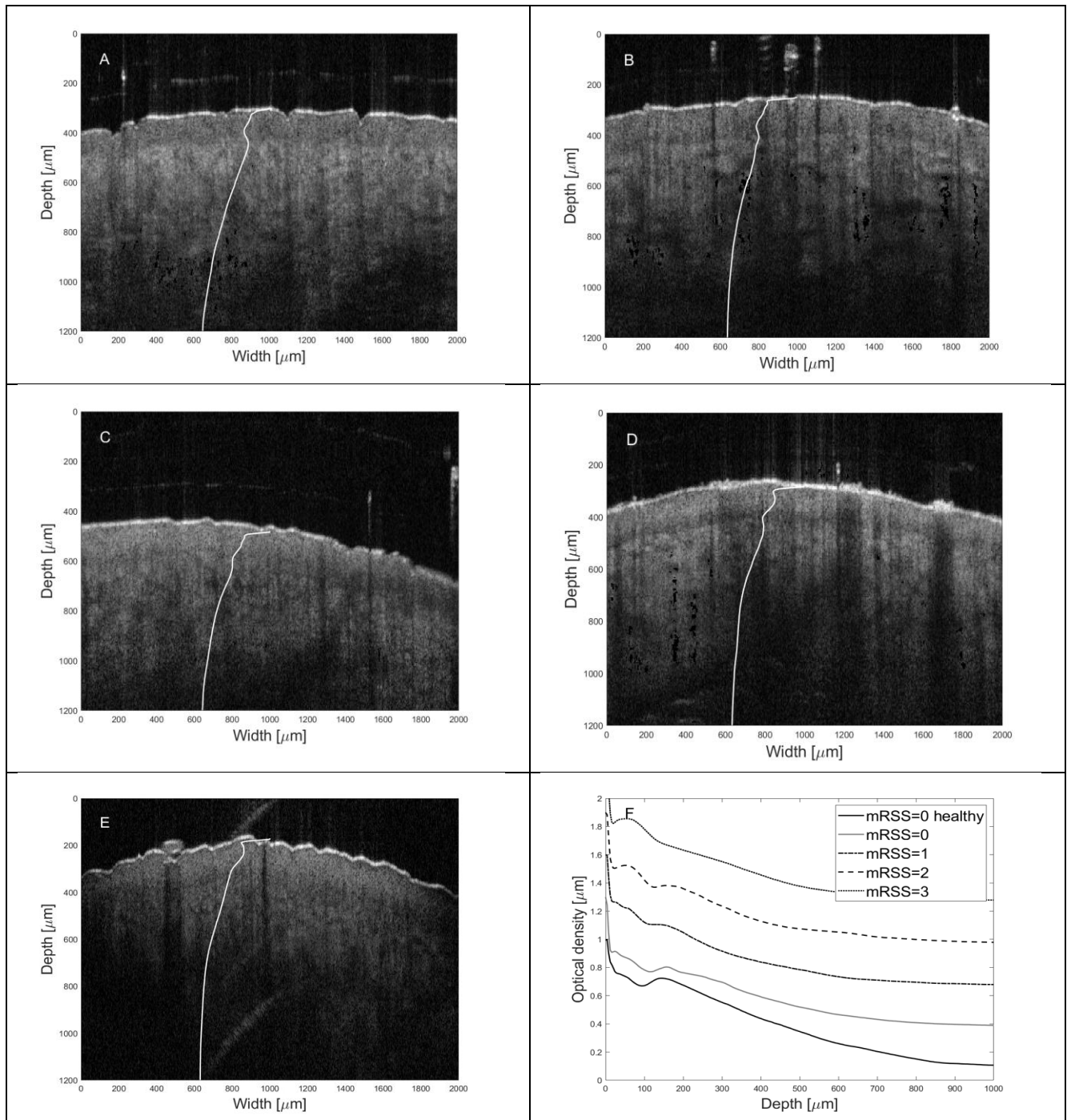
	SSc	Controls
Gender (Female/Male)	32/6	34/4
Age (years)	55 (16-79)	54,5 (26-83)
Disease duration from RP (years)	10 (1-15)	-
Disease duration from non-RP (years)	7 (0-20)	-
Disease subset (diffuse/limited)	10/28	-
ANA+	38	-
Topoisomerase+	6	-
ACA+	16	-
Mean mRSS (/51)	4 (0-20)	0

Abbreviations: ACA: anti-centromere antibody; ANA: antinuclear antibody; D/L: diffuse/limited; mRSS: modified Rodnan skin score; RP: Raynaud phenomenon; SSc: systemic sclerosis

QUALITATIVE COMPARISON

With both systems, we could observe the same significant differences between the images of the diseased skin and those of the normal skin. The main one was the darkness of the PD making the junction difficult to visualize from the underlying dermis. This difference seemed all the more striking as the clinical impairment was marked. Otherwise, the

epidermis seemed intact, contrasting with the rest of the structures by its brightness. Moreover, we noticed a loss of superficial folds associated with the rarefaction of skin appendages in involved skin. These observations were similar with the 2 systems although the sensitivity seemed superior with the Skintell®. (Figure 2 and supplementary figure 1)



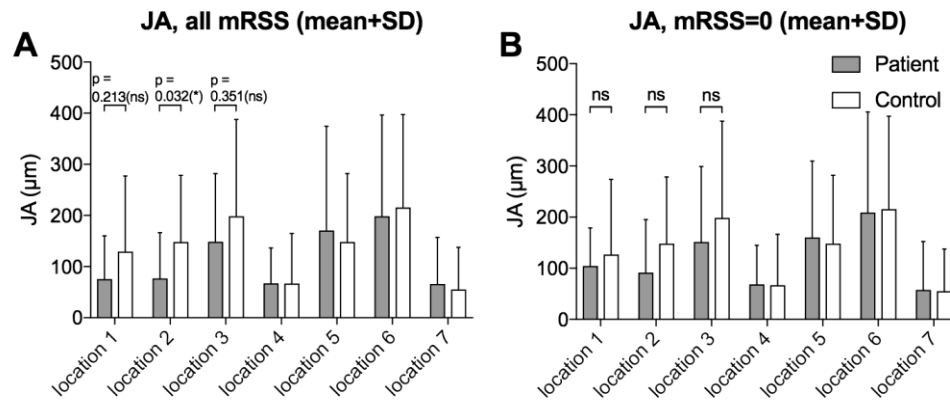
Supplementary Figure 1. Example of image processing with the Vivosight data set for location 2 for (A) a healthy volunteer (mRSS=0) and for SSc patients displaying a Rodnan score of (B) mRSS=0, (C) mRSS=1, (D) mRSS=2 and (E) mRSS=3. Insert F shows all the depth profiles displaced vertically for the sake of illustration.

Abbreviations: mRSS: modified Rodnan skin score

QUANTITATIVE COMPARISON

From the four Vivosight®-derived parameters evaluated, only the JA difference between patients and healthy controls appeared significant for the sole skin site 2 (patients, n=36: $77 \pm 89.6 \mu\text{m}$ (mean \pm SD); controls, n=38: $148.1 \pm 130.3 \mu\text{m}$; corrected P-value = 0.032), while mRSS proved to be very

significant to extremely significant (corrected P-values < 0.01) for all lesions according to their location (supplementary figure 2). JA significantly correlated with mRSS for skin site 1 (Spearman r [95%CI] = -0.564 [-0.7725 to -0.2447], P value = 0.0012). No correlation was observed for the other Vivosight® measurement sites.

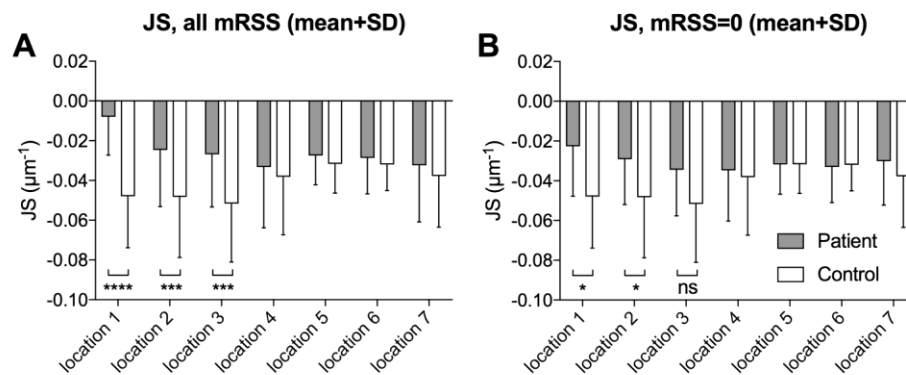


Supplementary Figure 2. A. Comparison of OCT-derived junction area (JA) at the 7 investigated locations, considering all mRSS. B. Same comparison when considering only the measurements where mRSS=0.

Abbreviations: JA: junction area; mRSS: modified Rodnan skin score; OCT: optical coherence tomography SD: standard deviation

The same tests performed on the quantitative parameters derived from the Skintell® images revealed the JS as the most relevant one, as can be seen in Table 2. In particular, JS was significantly lower in the first three imaged skin sites in SSc patients relative to controls (Supplementary figure 3) when compared to mRSS. At all the 7 imaging sites, JS performed better than mRSS.

The OD ratio between PD and epidermis in patients proved to be significantly lower as well in the first two skin sites (Table 2). In skin site 1 only, where the average mRSS was the highest, the normalized OD PD / OD epidermis revealed significantly lower in patients compared to healthy controls.



Supplementary Figure 3. A. Comparison of HD OCT-derived junction slope (JS) at the 7 investigated locations, considering all mRSS. B. Same comparison when considering only the measurements where mRSS=0.

Abbreviations: HD-OCT: high definition optical coherence tomography; JS: junction slope; mRSS: modified Rodnan skin score; SD: standard deviation

Table 2. Summary of statistically significant results from HD-OCT-derived quantitative parameters analysis the 7 anatomical skin sites.

Lesion	Metrics	Patients			Controls			corr. p
		Mean	SD	n	Mean	SD	n	
1	mRSS	1.405	1.212	36	0	0	38	< 0.0001
	JS (μm^{-1})	$-7.97 \cdot 10^{-3}$	$-19.3 \cdot 10^{-3}$	36	$-48 \cdot 10^{-3}$	$26 \cdot 10^{-3}$	38	< 0.0001
	(PD/Epi) OD	0.195	0.148	36	0.369	0.166	38	< 0.001
	Norm. PD OD	0.221	0.143	24	0.344	0.164	38	0.027
2	mRSS	0.972	1.207	36	0	0	37	< 0.0001
	JS (μm^{-1})	-0.0247	0.0285	36	-0.0483	0.0305	37	0.01

		Patients			Controls			
	(PD/Epi) OD	0.323	0.190	36	0.458	0.195	37	0.029
3	mRSS	0.778	1.098	36	0	0	37	< 0.001
	JS(μm^{-1})	-0.0269	0.0264	36	-0.0517	0.0294	37	0.003
4	mRSS	0.611	0.994	36	0	0	37	0.003
5	mRSS	0.556	0.939	36	0	0	37	0.006
6	mRSS	0.472	0.878	36	0	0	37	0.016
7	mRSS	0.694	1.009	36	0	0	37	< 0.001

Abbreviations: Epi: epidermis; HD-OCT: high definition optical coherence tomography; JS: junction slope; mRSS: modified Rodnan skin score; OD: optical density; PD: papillary dermis; SD: standard deviation; SSc: systemic sclerosis

A correlation was found between mRSS and Skintell® derived JS for all skin sites except skin site 4 (Table 3). As can be observed, correlation was the highest in the first measurement site.

Table 3. Summary of Spearman correlation r , 95% confidence interval and P values for HD-OCT derived JS (in μm^{-1}) with mRSS for 6 anatomical skin sites.

	site 1	site 2	site 3	site 5	site 6	site 7
Spearman r	0.709	0.428	0.424	0.382	0.361	0.397
95% CI min	0.570	0.214	0.210	0.162	0.138	0.181
95% CI max	0.809	0.602	0.600	0.566	0.550	0.577
P-value	< 0.0001	0.0001	0.0002	0.0008	0.0016	0.0004

Abbreviations: CI: confidence interval

ROC curves were computed for JA since it was the only significantly relevant quantitative parameter derived from the Vivosight® A-scan data, thereby enabling to classify patients with scleroderma. All patients were pooled, whatever their mRSS. The accuracy was poor for the second location (AUC [SD] = 0.68 [0.063], P-value=0.008), with a cutoff

value of 85.14 (sensitivity=69.4%, specificity=68.4%), while JA failed to classify patients and controls (AUC \leq 0.6) at all the other lesion locations. In comparison, the ROC curves associated to mRSS exhibited an accuracy ranging from good to fair and were all statistically significant (Table 4).

Table 4. Results of ROC curve analysis for mRSS, HD-OCT JS, and HD-OCT JS when considering only patients with mRSS=0, for the three first skin measurement location.

	Location 1			Location 2			Location 3		
	mRSS	JS (μm^{-1})	JS (μm^{-1}) (mRSS=0)	mRSS	JS (μm^{-1})	JS (μm^{-1}) (mRSS=0)	mRSS	JS (μm^{-1})	JS (μm^{-1}) (mRSS=0)
AUC	0.84	0.91	0.78	0.74	0.76	0.71	0.71	0.74	0.70
SD	0.050	0.035	0.086	0.060	0.058	0.079	0.062	0.058	0.073
P-value	<0.0001	<0.0001	0.005	<0.001	<0.0001	0.009	0.002	0.003	0.033
Cutoff	>0.5	-0.0188	-0.0245	>0.5	-0.0274	-0.0274	>0.5	-0.0415	0.0415
Se	67.6%	83.8%	72.7%	47.2%	70.3%	63.2%	41.67%	71.4%	71.4%
Sp	100%	87.2%	79.5%	100%	84.2%	84.2%	100%	65.8%	65.8%

Abbreviations: AUC: area under the curve; JS: junction slope; mRSS: modified Rodnan skin score; SD: standard deviation; Se: sensitivity; Sp: specificity.

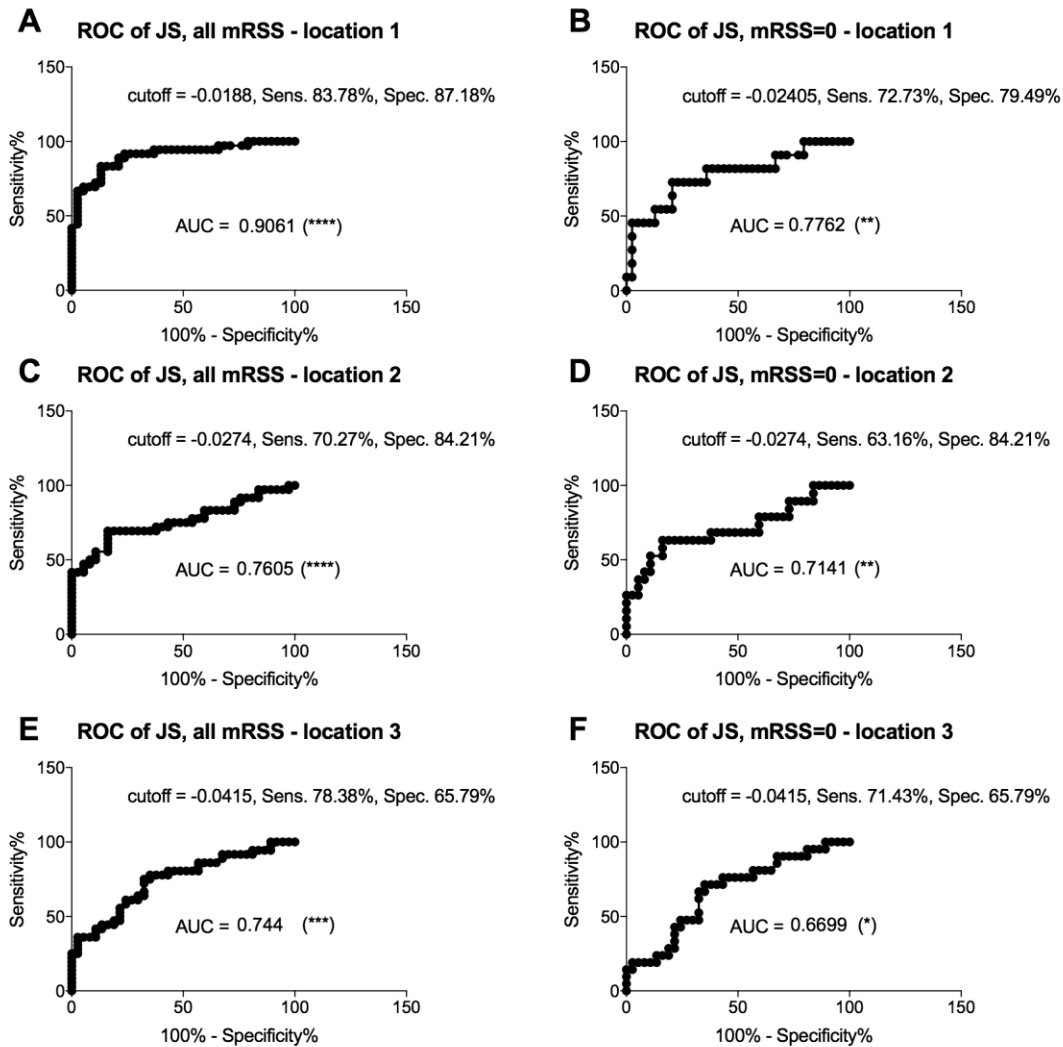
We further investigated whether JA would be able to classify patients with mRSS=0. In this view, only patients with mRSS=0 were kept in the patient's group for comparison against control subjects. Accuracy was poor for locations 1 and 2, but not significant (location 1: AUC [SD]=0.65 (0.079), P-value=0.168; location 2: AUC=0.65 (0.077), P-

value=0.063), while JA just failed at all the other locations.

Similar ROC curves were computed and analyzed for JS, the most relevant quantitative Skintell®-derived parameter, as can be seen in supplementary figure 4. When considering

classification of patients, whatever their mRSS, JS proved to perform better than mRSS in a challenge with control subjects, at locations 1, 2 and 3, at least. At location 1, accuracy was excellent when using a cutoff of $JS = -0.0188 \mu\text{m}^{-1}$. For locations 2 and 3, accuracy was fair, and slightly higher than

mRSS. Additionally, JS showed a fairly good accuracy in discriminating between patients and control subjects when considering only patients with $mRSS = 0$ (supplementary figure 4.B, D, and F). Indeed, in location 1, accuracy was fair, whereas in locations 2 and 3, accuracy was poor.



Supplementary Figure 4. ROC curves of HD OCT-derived JS. Top, middle, and bottom row depict ROC curves for location 1, 2, and 3, respectively. On the left (A, C, E), the ROC curves have been obtained whatever the mRSS. On the right (B, D, F), the corresponding curve when only measurements where $mRSS = 0$ are considered. Cutoff values are in μm^{-1} .

Abbreviations: AUC: Area under the curve; HD-OCT: high-definition optical coherence tomography; JS: junction slope; mRSS: modified Rodnan skin score; ROC: Receiver Operator Characteristic

Discussion

Up to now, mRSS remains the only gold standard for the semi-quantitative assessment of the skin fibrosis, both in daily practice and clinical trials^{10-13,38}. However, despite its convenience and reproducibility, certain drawbacks remain due to the subjectivity inherent to operator skills and interpretations^{14,15}. Although subjective assessment of the cutaneous involvement imaged by both OCT systems was not the main goal of our study,

qualitative evaluation and comparison enabled to further assess the morphological changes in SSc skin compared to normal skin. We observed that the dermis appeared much darker and the DEJ less identifiable as the severity of disease increases. This decreased reflectiveness may be caused, in part, by dermal edema and thickening of skin related to SSc. Moreover, thickening and horizontalization of collagen fibers may be responsible for decreasing the backscattering of the light and therefore the

brightness of the dermis. Moreover, the other observations were consistent with the histological characteristics already known of the SSc skin, namely the loss of superficial skin folds and the rarefaction of the skin appendages.

In the light of the above, we expected the fibrosis in the upper dermis would increase the optical scattering (hence decreasing the backscattered light), thereby resulting in an altered measured JS by OCT. Similarly, the fibrosis in the papillary dermis would diminish JA. As such, we then performed quantitative assessment of skin with OCT to evaluate the morphological changes observed in the skin of SSc patients. We could not observe significant changes in JA (except for the second studied location) in SSc patients and controls. These results differ from those described by the study of Abignano et al³⁰. This discrepancy could be related to the fact that the latter study included Vivosight® images taken at distal locations of the body, namely hand and forearm, where sclerosis changes occur earlier and stronger in the disease course.

On the other hand, Skintell® images using JS parameter showed significant changes for the first three locations in SSc patients compared to controls. A very interesting discovery of our work is the ability of JS images to objectify morphological changes in clinically uninvolved SSc skin compared to normal skin. However, we were not able to show significant differences in JS for the 4th to 7th locations. Since cutaneous involvement in SSc undergoes a distal-proximal progression, it may be due to the smallest proportion of affected skin as we move up proximally resulting in less rapidly significant differences by statistical effect. Furthermore, a significant correlation was found between mRSS and Skintell®-derived JS for all skin sites (except skin site 4). This technology could not only help to make the diagnosis but also offer an objective tool to assess the severity of the disease with the advantage to be user independent. It could permit to follow the evolution of the disease and/or the effectiveness of a treatment more precisely and quantitatively. Moreover, studies using this objective methodology would be comparable to each other and so, it could offer the possibility to realize meta-analysis increasing relevance of clinical research.

The results with JS for location 1 are particularly noteworthy and promising because they suggest that it would be possible to make an early diagnosis of SSc patients without clinical manifestations of skin involvement, i.e., with mRSS=0, with good precision, sensitivity and specificity. For the patient, early diagnosis offers the possibility to initiate early treatment and better prognosis. For these patients

with mRSS=0, we were not able to show significant difference in 3th to 7th locations. As already discussed, distal clinically uninvolved skin may include more subclinical involvement whereas proximal locations may be real uninvolved skin.

Our study has several limitations. First, morphological changes observed with imaging techniques were not compared with histology. Indeed, no cutaneous biopsy was taken to avoid the fore-mentioned potential consequences. Second, only one investigator assessed mRSS despite notable inter variability inherent in this score. Third, quantitative variables – namely JA for Vivosight® and JS for Skintell®- comparing involved skin to healthy skin were not the same according to the selected imaging technique. Finally, images were only taken at 7 of the 17 mRSS. The DEJ becomes increasingly difficult to identify as the mRSS score increases as demonstrated with JA and to a significantly lesser extent with JS. Beyond the quantitative analysis of the DEJ with JS and JA, it would be very interesting to further analyze the upper dermis part in the OCT curves with a yet to be identified quantitative parameter that would be optimally sensitive to what is visually evident.

Taken together, our study highlight the potential of HD-OCT to detect morphological changes in SSc patients, making it a promising technology for the early non-invasive diagnosis of patients suffering from SSc. In addition, it constitutes a more objective and relevant tool for skin examination and follow-up than mRSS. From a practical point of view, examination was quick (less than 5 minutes), painless, and well tolerated, offering it as a practical tool easy to implement in both routine clinical practice and clinical trials. However, further studies are needed to better clarify and confirm the role of HD-OCT in the early diagnosis and management SSc patients.

Conclusion

Our study indicates the potential contribution of HD-OCT in the early diagnosis and in the management of SSc patients. HD-OCT constitutes a non-invasive imaging technique that can be easily implemented in routine clinical practice and clinical trials. In addition, it represents a more objective and unbiased tool than mRSS. In the near future, HD-OCT could be a validated tool for the diagnosis and assessment of skin involvement in SSc.

Conflicts of interest: The authors disclose no conflicts of interest and no financial interests

Funding: No specific funding was received from any bodies in the public, commercial or not-for-

profit sectors to carry out the work described in this article.

Acknowledgment: Prof M.S Soyfoo is a bursary of the King Baudouin foundation for rheumatology.

Ethics: The authors state that the study complies with the Declaration of Helsinki. The locally appointed ethics committee of Erasmus Hospital has approved the research protocol.

Abbreviations

ACR/EULAR: American College of Rheumatology/European League Against Rheumatism
AUC: Area under the curve

dcSSc: diffuse cutaneous SSc
DEJ: dermal-epidermal junction
ET: epidermis thickness
HD: high-definition
HFUS: high frequency ultrasound
JA: junction area
JOD: junction OD
JS: junction slope
JT: junction thickness
lcSSc: limited cutaneous SSc
mRSS: modified Rodnan skin score
OCT: optical coherence tomography
OD: optical density
PD: papillary dermis
ROC: Receiver Operator Characteristic
SD: standard deviation
SSc: systemic sclerosis

References

1. Varga J, Abraham D. Systemic sclerosis: a prototypic multisystem fibrotic disorder. *J Clin Invest.* Mar 2007;117(3):557-67. doi:10.1172/JCI31139
2. Denton CP, Khanna D. Systemic sclerosis. *Lancet.* Oct 7 2017;390(10103):1685-1699. doi:10.1016/S0140-6736(17)30933-9
3. Volkman ER, Andreasson K, Smith V. Systemic sclerosis. *Lancet.* Jan 28 2023;401(10373):304-318. doi:10.1016/S0140-6736(22)01692-0
4. Desbois AC, Cacoub P. Systemic sclerosis: An update in 2016. *Autoimmun Rev.* May 2016;15(5):417-26. doi:10.1016/j.autrev.2016.01.007
5. Nihtyanova SI, Schreiber BE, Ong VH, Rosenberg D, Moizadeh P, Coghlan JG, et al. Prediction of pulmonary complications and long-term survival in systemic sclerosis. *Arthritis Rheumatol.* Jun 2014;66(6):1625-35. doi:10.1002/art.38390
6. LeRoy EC, Medsger TA, Jr. Criteria for the classification of early systemic sclerosis. *J Rheumatol.* Jul 2001;28(7):1573-6.
7. Steen VD, Medsger TA. Changes in causes of death in systemic sclerosis, 1972-2002. *Ann Rheum Dis.* Jul 2007;66(7):940-4. doi:10.1136/ard.2006.066068
8. Elhai M, Meune C, Boubaya M, Avouac J, Hachulla E, Balbir-Gurman A, et al. Mapping and predicting mortality from systemic sclerosis. *Ann Rheum Dis.* Nov 2017;76(11):1897-1905. doi:10.1136/annrheumdis-2017-211448
9. Khanna D, Furst DE, Clements PJ, Allanore Y, Baron M, Czirjak L, et al. Standardization of the modified Rodnan skin score for use in clinical trials of systemic sclerosis. *J Scleroderma Relat Disord.* Jan-Apr 2017;2(1):11-18. doi:10.5301/jsrd.5000231
10. Shand L, Lunt M, Nihtyanova S, Hoseini M, Silman A, Black CM, et al. Relationship between change in skin score and disease outcome in diffuse cutaneous systemic sclerosis: application of a latent linear trajectory model. *Arthritis Rheum.* Jul 2007;56(7):2422-31. doi:10.1002/art.22721
11. Steen VD, Medsger TA, Jr. Improvement in skin thickening in systemic sclerosis associated with improved survival. *Arthritis Rheum.* Dec 2001;44(12):2828-35. doi:10.1002/1529-0131(200112)44:12<2828::aid-art470>3.0.co;2-u
12. Domsic RT, Rodriguez-Reyna T, Lucas M, Fertig N, Medsger TA, Jr. Skin thickness progression rate: a predictor of mortality and early internal organ involvement in diffuse scleroderma. *Ann Rheum Dis.* Jan 2011;70(1):104-9. doi:10.1136/ard.2009.127621
13. Wu W, Jordan S, Graf N, de Oliveira Pena J, Curram J, Allanore Y, et al. Progressive skin fibrosis is associated with a decline in lung function and worse survival in patients with diffuse cutaneous systemic sclerosis in the European Scleroderma Trials and Research (EUSTAR) cohort. *Ann Rheum Dis.* May 2019;78(5):648-656. doi:10.1136/annrheumdis-2018-213455
14. Clements P, Lachenbruch P, Siebold J, White B, Weiner S, Martin R, et al. Inter and intraobserver variability of total skin thickness score (modified Rodnan TSS) in systemic sclerosis. *J Rheumatol.* Jul 1995;22(7):1281-5.
15. Clements PJ, Lachenbruch PA, Seibold JR, Zee B, Steen VD, Brennan P, et al. Skin thickness score in systemic sclerosis: an assessment of interobserver variability in 3 independent studies. *J Rheumatol.* Nov 1993;20(11):1892-6.
16. Hachulla E, Agard C, Allanore Y, Avouac J, Bader-Meunier B, Belot A, et al. French recommendations for the management of systemic sclerosis. *Orphanet J Rare Dis.* Jul 26 2021;16(Suppl 2):322. doi:10.1186/s13023-021-01844-y
17. Fueyo-Casado A, Campos-Munoz L, Pedraz-Munoz J, Conde-Taboada A, Lopez-Bran E. Nail fold dermoscopy as screening in suspected connective tissue diseases. *Lupus.* Jan 2016;25(1):110-1. doi:10.1177/0961203315605369
18. de Oliveira MFC, Leopoldo VC, Pereira KRC, de Moraes DA, Dias JBE, Goncalves MS, et al. Durometry as an alternative tool to the modified Rodnan's skin score in the assessment of diffuse systemic sclerosis patients: a cross-sectional study. *Adv Rheumatol.* Sep 21 2020;60(1):48. doi:10.1186/s42358-020-00152-6
19. Vanhaecke A, Verschuere S, Vilela V, Heeman L, Cutolo M, Smith V. Durometry in SSc: The hard facts. A systematic literature review and additional pilot study. *Rheumatology (Oxford).* May 14 2021;60(5):2099-2108. doi:10.1093/rheumatology/keab028
20. Moore TL, Lunt M, McManus B, Anderson ME, Herrick AL. Seventeen-point dermal ultrasound scoring system--a reliable measure of skin thickness in patients with systemic sclerosis. *Rheumatology (Oxford).* Dec 2003;42(12):1559-63. doi:10.1093/rheumatology/keg435
21. Vanhaecke A, Cutolo M, Heeman L, Vilela V, Deschepper E, Melsens K, et al. High frequency ultrasonography: reliable tool to measure skin

- fibrosis in SSC? A systematic literature review and additional pilot study. *Rheumatology (Oxford)*. Dec 24 2021;61(1):42-52. doi:10.1093/rheumatology/keab462
22. Vos MHE, Nguyen KP, Van Erp PEJ, Van de Kerkhof PCM, Driessen RJB, Peppelman M. The value of (video)dermoscopy in the diagnosis and monitoring of common inflammatory skin diseases: a systematic review. *Eur J Dermatol*. Oct 1 2018;28(5):575-596. doi:10.1684/ejd.2018.3396
 23. Flower VA, Barratt SL, Hart DJ, Mackenzie AB, Shipley JA, Ward SG, et al. High frequency ultrasound assessment of systemic sclerosis skin involvement: intra-observer repeatability and relationship with clinician assessment and dermal collagen content. *J Rheumatol*. Nov 1 2020;doi:10.3899/jrheum.200234
 24. Naredo E, Pascua J, Damjanov N, Lepri G, Gordaliza PM, Janta I, et al. Performance of ultra-high-frequency ultrasound in the evaluation of skin involvement in systemic sclerosis: a preliminary report. *Rheumatology (Oxford)*. Jul 1 2020;59(7):1671-1678. doi:10.1093/rheumatology/kez439
 25. Huang D, Swanson EA, Lin CP, Schuman JS, Stinson WG, Chang W, et al. Optical coherence tomography. *Science*. Nov 22 1991;254(5035):1178-81. doi:10.1126/science.1957169
 26. Di Y, Ye JJ. [Application of optical coherence tomography angiography in ophthalmology]. *Zhonghua Yan Ke Za Zhi*. Jan 11 2017;53(1):65-72. doi:10.3760/cma.j.issn.0412-4081.2017.01.013
 27. Shah R. Optical coherence tomography-guided PCI. *Lancet*. Apr 22 2017;389(10079):1607. doi:10.1016/S0140-6736(17)31017-6
 28. Olsen J, Themstrup L, Jemec GB. Optical coherence tomography in dermatology. *G Ital Dermatol Venereol*. Oct 2015;150(5):603-15.
 29. Levine A, Wang K, Markowitz O. Optical Coherence Tomography in the Diagnosis of Skin Cancer. *Dermatol Clin*. Oct 2017;35(4):465-488. doi:10.1016/j.det.2017.06.008
 30. Heibel HD, Hooley L, Cockerell CJ. A Review of Noninvasive Techniques for Skin Cancer Detection in Dermatology. *Am J Clin Dermatol*. Aug 2020;21(4):513-524. doi:10.1007/s40257-020-00517-z
 31. Ha L, Hundt JE. Optical coherence tomography for fast bedside imaging, assessment and monitoring of autoimmune inflammatory skin diseases? *J Dtsch Dermatol Ges*. Sep 2020;18(9):937-942. doi:10.1111/ddg.14266
 32. Abignano G, Aydin SZ, Castillo-Gallego C, Liakouli V, Woods D, Meekings A, et al. Virtual skin biopsy by optical coherence tomography: the first quantitative imaging biomarker for scleroderma. *Ann Rheum Dis*. Nov 2013;72(11):1845-51. doi:10.1136/annrheumdis-2012-202682
 33. Pires NSM, Dantas AT, Duarte A, Amaral MM, Fernandes LO, Dias TJC, et al. Optical coherence tomography as a method for quantitative skin evaluation in systemic sclerosis. *Ann Rheum Dis*. Mar 2018;77(3):465-466. doi:10.1136/annrheumdis-2016-210875
 34. Liu CH, Assassi S, Theodore S, Smith C, Schill A, Singh M, et al. Translational optical coherence elastography for assessment of systemic sclerosis. *J Biophotonics*. Dec 2019;12(12):e201900236. doi:10.1002/jbio.201900236
 35. Boone M, Jemec GB, Del Marmol V. High-definition optical coherence tomography enables visualization of individual cells in healthy skin: comparison to reflectance confocal microscopy. *Exp Dermatol*. Oct 2012;21(10):740-4. doi:10.1111/j.1600-0625.2012.01569.x
 36. van den Hoogen F, Khanna D, Fransen J, Johnson SR, Baron M, Tyndall A, et al. 2013 classification criteria for systemic sclerosis: an American college of rheumatology/European league against rheumatism collaborative initiative. *Ann Rheum Dis*. Nov 2013;72(11):1747-55. doi:10.1136/annrheumdis-2013-204424
 37. LeRoy EC, Black C, Fleischmajer R, Jablonska S, Krieg T, Medsger TA, Jr., et al. Scleroderma (systemic sclerosis): classification, subsets and pathogenesis. *J Rheumatol*. Feb 1988;15(2):202-5.
 38. Clements PJ, Hurwitz EL, Wong WK, Seibold JR, Mayes M, White B, et al. Skin thickness score as a predictor and correlate of outcome in systemic sclerosis: high-dose versus low-dose penicillamine trial. *Arthritis Rheum*. Nov 2000;43(11):2445-54. doi:10.1002/1529-0131(200011)43:11<2445::AID-ANR11>3.0.CO;2-Q